AAS 14-237

F AND G TAYLOR SERIES SOLUTIONS TO THE CIRCULAR RESTRICTED THREE BODY PROBLEM

Etienne Pellegrini*, and Ryan P. Russell†

The Circular Restricted Three-Body Problem is solved using an extension to the classic F and G Taylor series. The Taylor series coefficients are developed using exact recursion formulas, which are implemented via symbolic manipulation software. In addition, different time transformations are studied in order to obtain an adapted discretization for the three-body problem. The resulting propagation method is compared to a conventional numerical integration method, the Runge-Kutta-Fehlberg integrator, on a set of test scenarios designed to qualitatively represent the different types of three-body motion. The series solution is demonstrated to have comparable performance to the conventional integrator, when considering a variety of circumstances, such as the independent variable, error tolerance, orbit characteristics, and integration scheme. In the variable-step case, for low-fidelity applications, such as preliminary design of trajectories, the F and G series with no time transformation are shown to be two to three times faster than the conventional integrator in all cases, when selecting an appropriate order. In the fixed-step case, the Sundman time transformations are demonstrated to reduce the number of steps required for convergence by one or more orders of magnitude. This improved discretization confirms the value of regularization in the restricted three-body problem, and suggests the utility of fixed-step integration using Sundman transformed equations of motion.

1 INTRODUCTION

The Circular Restricted Three-Body Problem (CRTBP) is a well-known astrodynamics problem, useful for a variety of applications, from modeling the Earth-Moon system to the exploitation of invariant manifolds for satellite tour design.[1,2,3] The CRTBP model consists of two masses in circular orbits around each other, and a massless particle influenced by both. An extensive description of the CRTBP can be found in Ref. 4, and the equations of motion are presented in Subsection 2.1. Like other astrodynamics problems, the equations of motion of the CRTBP can be solved using a variety of methods, including Runge-Kutta, multistep, symplectic, collocation, and Taylor series methods.[5,6] The latter have been demonstrated to have several advantages over other integration methods, in particular because they allow for variable-order integration, natural interpolation between steps, and a simple estimation of the truncation error.[7,8] Therefore, series solutions have long been of interest in the context of the CRTBP. In particular, several authors have developed recursive power series, as they can be used to arbitrary order. Steffensen[9] first published a recursive power series solution to both the general and the restricted three-body problem. Rabe[10] applied his method to the computation of periodic Trojan orbits. Fehlberg,[8] Deprit and Price,[11] and Broucke[12] also studied and used power series methods, which have been shown to compare favorably to traditional numerical methods.[13,14]

The present work aims at solving the equations of motion of the 3D CRTBP using a different set of recursive Taylor series. Here, the classic F and G series, Taylor expansions of Lagrange's f and g coefficients,[15] are extended to the resctricted three-body motion. The recursion formulas for the obtention of the F and G series have been developed for a variety of celestial mechanics problems, such as the two-body problem,[16,17] the N-body problem,[18] and more recently as a solution to the Stark problem.[19] In the latter case, the extended F and G Stark series were demonstrated to be significantly faster than a fixed-step Runge-Kutta-Fehlberg

*Graduate Student, Aerospace Engineering and Engineering Mechanics, The University of Texas at Austin, Austin, TX
†Assistant Professor, Aerospace Engineering and Engineering Mechanics, The University of Texas at Austin, Austin, TX

(RKF) integrator of order 8. Therefore, a main motivation for the present work is to examine the efficiency of a similar method for the propagation of the CRTBP. Automated trajectory design methods stand to benefit from using three-body dynamics, and a fast integration technique is essential for optimization algorithms. Moreover, Jorba and Zou[14] demonstrated that their variable-order Taylor series solution had performance comparable to `dop853`, a variable-order explicit Runge-Kutta integrator of order 8. The main objective of the current paper is to develop and test the F and G Taylor series solution to the CRTBP.

As part of the formulation, regularization techniques based on the classic Sundman transformation are implemented and examined.[20] Szebehely[4] extensively describes and justifies the need for regularization methods in the CRTBP, as close approaches between bodies are common and lead to singularities in the limit of collisions. In particular, Szebehely describes regularization techniques by Birkhoff,[21] Lemaitre,[22] and Thiele and Burrau,[23,24] and gives a historical survey of regularization methods. However, in the current study, only basic modifications of the Sundman transformation will be considered.

The results are presented for the application of both the F and G series solution and the Sundman type regularization techniques to the CRTBP. The derivation of the recursive coefficients for the series is shown in Section 2. The numerical results presented in Section 3 demonstrate the successful integration of the CRTBP via F and G type series. The performance of the newly introduced integration method is compared to that of a conventional numerical integrator. An eighth order Runge-Kutta-Fehlberg integrator is chosen as the benchmark integrator, in both its fixed-step and variable-step variants, which will be designated by RKF8 and RKF(7)8 respectively. In addition, the performance of the Sundman type regularization techniques is examined.

2 FORMULATION OF THE SERIES SOLUTION

This section presents the development of the recursive formulas necessary for the computation of the F and G CRTBP series. The classic F and G series are extended to the propagation of the 3D CRTBP and to include Sundman type transformations.

2.1 The Circular Restricted Three-Body Problem

The CRTBP is a well-known celestial mechanics problem which consists of two masses in circular orbits, and a massless particle whose motion is influenced by both masses. The CRTBP is described extensively by Szebehely.[4] For the derivation of the F and G series, the equations of motion are expressed in the inertial frame (see Subsection 2.3). The inertial frame formulation is preferred in the context of obtaining the recursion equations. Moreover, many advanced design tools, such as Mystic, express the CRTBP in the inertial frame.[25] In the inertial formulation, explicit knowledge of the states of the two masses is also necessary. The augmented state vector, including all three bodies, is formed as:

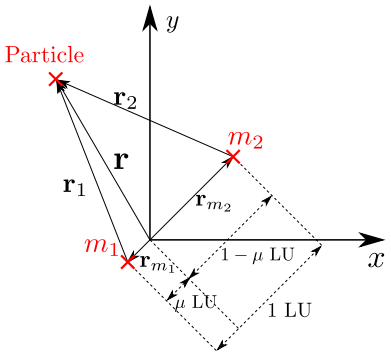

Figure 1: Sketch of the inertial frame CRTBP

$$\mathbf{X} = \left[\mathbf{r}^T\ \mathbf{v}^T\ \mathbf{r}_{m_1}^T\ \mathbf{v}_{m_1}^T\ \mathbf{r}_{m_2}^T\ \mathbf{v}_{m_2}^T\right]^T \tag{1}$$

where $\mathbf{r}$, $\mathbf{v}$ are the position and velocity of the massless particle in an inertial frame centered at the barycenter of the system; $\mathbf{r}_{m_i}$, $\mathbf{v}_{m_i}$ are the position and velocity of m_i, where m_1 is the primary (the heavier mass) and m_2 the secondary (the lighter mass, see Fig. 1). The units are all normalized as shown in Eq. (7) to (9) and

will be noted LU, TU, MU (Length Unit, Time Unit, Mass Unit, respectively).

$$\dot{\mathbf{X}} = \frac{d\mathbf{X}}{dt} = \begin{bmatrix} \mathbf{v} \\ -\frac{Gm_1}{r_1^3}\mathbf{r_1} - \frac{Gm_2}{r_2^3}\mathbf{r_2} \\ \mathbf{v}_{m_1} \\ -\frac{Gm_2}{r_{m_1}}\mathbf{r}_{m_1} \\ \mathbf{v}_{m_2} \\ -\frac{Gm_1}{r_{m_2}}\mathbf{r}_{m_2} \end{bmatrix} \tag{2}$$

By definition (see Fig. 1):

$$\mathbf{r}_1 = \mathbf{r} - \mathbf{r}_{m_1} \tag{3}$$
$$\mathbf{r}_2 = \mathbf{r} - \mathbf{r}_{m_2} \tag{4}$$
$$\mathbf{r}_{m_2} = -\frac{r_{m_2}}{r_{m_1}}\mathbf{r}_{m_1} = -c\mathbf{r}_{m_1} \tag{5}$$
$$\mathbf{v}_{m_2} = -c\mathbf{v}_{m_1} \tag{6}$$

with $c = \frac{r_{m_2}}{r_{m_1}}$. Moreover, the standard normalization of the CRTBP gives:

$$Gm_1 + Gm_2 \equiv 1 \text{ LU}^3/\text{TU}^2 \tag{7}$$
$$r_{m_1} + r_{m_2} \equiv 1 \text{ LU} \tag{8}$$
$$\omega \equiv 1 \text{ rad/TU} \tag{9}$$

where ω is the system's angular velocity. With $\mu = \frac{m_2}{m_1+m_2}$, those relations become:

$$Gm_1 = 1 - \mu \text{ LU}^3/\text{TU}^2 \tag{10}$$
$$Gm_2 = \mu \text{ LU}^3/\text{TU}^2 \tag{11}$$
$$r_{m_1} = \mu \text{ LU} \tag{12}$$
$$r_{m_2} = 1 - \mu \text{ LU} \tag{13}$$
$$\omega = 1 \text{ rad/TU} \tag{14}$$

Using Eq. (3) to (14), the location of the secondary can be expressed in terms of the primary, and the state vector can be simplified: $\mathbf{X} = \begin{bmatrix}\mathbf{r}^T & \mathbf{v}^T & \mathbf{r}_{m_1}^T & \mathbf{v}_{m_1}^T\end{bmatrix}^T$. The equations of motion become:

$$\dot{\mathbf{X}} = \begin{bmatrix} \mathbf{v} \\ p\mathbf{r} + q\mathbf{r}_{m_1} \\ \mathbf{v}_{m_1} \\ -\mathbf{r}_{m_1} \end{bmatrix} \text{ with } \begin{cases} p &= \left(-\frac{1-\mu}{r_1^3} - \frac{\mu}{r_2^3}\right) \\ q &= \left(\frac{1-\mu}{r_1^3} - \frac{1-\mu}{r_2^3}\right) \end{cases} \tag{15}$$

In the case of the Circular RTBP, the two masses m_1 and m_2 are in circular orbits around each other. Position and velocity of m_1, when necessary, are simply computed by rotation:

$$\mathbf{r}_{m_1}(t) = \begin{bmatrix} \cos(t-t_0) & -\sin(t-t_0) & 0 \\ \sin(t-t_0) & \cos(t-t_0) & 0 \\ 0 & 0 & 1 \end{bmatrix} \mathbf{r}_{m_1,0} \; ; \quad \mathbf{v}_{m_1}(t) = \begin{bmatrix} \cos(t-t_0) & -\sin(t-t_0) & 0 \\ \sin(t-t_0) & \cos(t-t_0) & 0 \\ 0 & 0 & 1 \end{bmatrix} \mathbf{v}_{m_1,0} \tag{16}$$

Finally, the equations of motion to be solved in this paper are:

$$\dot{\mathbf{X}} = \begin{bmatrix} \dot{\mathbf{r}} \\ \mathbf{v} \end{bmatrix} = \begin{bmatrix} \mathbf{v} \\ p\mathbf{r} + q\mathbf{r}_{\mathbf{m_1}} \end{bmatrix} \tag{17}$$

2.2 Sundman transformation

The Sundman transformation is a regularization of the equations of motion with the aim to avoid singularities due to collisions of attracting bodies. It was first developed by Karl F. Sundman in 1912 for the three-body problem.[20] The classic Sundman transformation consists of a change of the independent variable from time t to τ given by:

$$dt = r\, d\tau \tag{18}$$

The Sundman transformation has been proven to analytically suppress singularities for both the two-body and three-body problems.[26] It also improves the performance of integration techniques for the two-body problem.[27,28] However, Szebehely[4] shows that the use of a simple regularization technique, while analytically improving the problem, also results in an increased complexity of the equations of motion, which may degrade computational performance. In order to improve the numerical behavior of the equations of motion, more complicated regularization transformations have been introduced.[21,22,23,24,29] In the present development, only the simple Sundman type transformations are considered, leaving other regularization techniques for future work. The three transformations considered are regularizations of close approaches to m_1, m_2, or both. These can be written as $dt = s(\mathbf{r}, \mathbf{r}_{m_1})d\tau = s\, d\tau$ where $s = r_1 = \|\mathbf{r} - \mathbf{r}_{m_1}\|$, $s = r_2 = \|\mathbf{r} + c\mathbf{r}_{m_1}\|$ or $s = r_1 r_2 = \|\mathbf{r} - \mathbf{r}_{m_1}\|\|\mathbf{r} + c\mathbf{r}_{m_1}\|$, respectively. Keeping time as the independent variable (no Sundman transformation) is equivalent to using a Sundman transformation with $s = 1$. Reference 19 presents the application of the Sundman type transformations to the equations of motion. The main result is:

$$\begin{cases} \mathbf{X}' = \dfrac{d\mathbf{X}}{d\tau} = \dfrac{d\mathbf{X}}{dt}\dfrac{dt}{d\tau} = s\dot{\mathbf{X}} \\ \dfrac{dt}{d\tau} = s \end{cases} \tag{19}$$

where x' and $\dot{x}$ designate differentiations of the dummy variable x with respect to τ and time, respectively. When applying the transformation to Eq. (17), the equations of motion become:

$$\begin{cases} \mathbf{X}' = \begin{bmatrix} s\mathbf{v} \\ s(p\mathbf{r} + q\mathbf{r}_{m_1}) \end{bmatrix} \\ t' = s \end{cases} \tag{20}$$

2.3 Recursion formulas

The Lagrange coefficients f and g are a well-known solution method to the two-body problem.[15] The position and velocity vectors at τ are decomposed in the basis formed by position and velocity at τ_0:

$$\begin{aligned} \mathbf{r}(\tau) &= f\mathbf{r}(\tau_0) + g\mathbf{v}(\tau_0) \\ \mathbf{v}(\tau) &= \dot{f}\mathbf{r}(\tau_0) + \dot{g}\mathbf{v}(\tau_0) \end{aligned} \tag{21}$$

These expressions are valid for the two-body problem. In the case of the 3D CRTBP, at least one more basis vector is necessary, since the motion is not confined to the initial plane. The authors have studied the development of the series for a variety of basis vectors, and a variety of formulations of the problem (including the propagation in the rotating frame), but the resulting expressions lead to less convenient sets of recursion formulas. The best option of those considered uses four vectors to span the full space: $\mathbf{r}_0$, $\mathbf{v}_0$, $\mathbf{r}_{m_1,0}$, and $\mathbf{v}_{m_1,0}$. The space can not be spanned under all circumstances, using any three of the vectors. A fourth vector is potentially redundant, however, is necessary to ensure the recursions. In addition, the use of the Sundman transformation requires the tracking of time as a dependent variable, as shown in Eq. (20), which makes a fifth series necessary to solve the problem. The solution presented in this paper will therefore extend the classic F and G formulation to five series. However, for legacy purposes the set of five series will be called "F and G CRTBP series".

The position and velocity vectors have to be expressed as Taylor series in the independent variable τ. For order N, the position vector $\mathbf{r}$ at $\tau = \tau_0 + \Delta\tau$ can be written as:

$$\mathbf{r} \simeq \sum_{n=0}^{N} \left.\frac{d^n \mathbf{r}}{d\tau^n}\right|_{\tau_0} \frac{\Delta\tau^n}{n!} \tag{22}$$

Since the set of four vectors $\mathbf{r}_0$, $\mathbf{v}_0$, $\mathbf{r}_{m_1,0}$, $\mathbf{v}_{m_1,0}$ forms a basis of the 3D space, the consecutive derivatives of r in Eq. (22) can be expressed in this basis:

$$\left.\frac{d^n \mathbf{r}}{d\tau^n}\right|_{\tau_0} = F_n|_{\tau_0}\mathbf{r}_0 + G_n|_{\tau_0}\mathbf{v}_0 + A_n|_{\tau_0}\mathbf{r}_{m_1,0} + B_n|_{\tau_0}\mathbf{v}_{m_1,0} \tag{23}$$

Equation (23) is plugged in Eq. (22):

$$\begin{aligned}\mathbf{r} &\simeq \sum_{n=0}^{N}\left[F_n|_{\tau_0}\frac{\Delta\tau^n}{n!}\right]\mathbf{r}_0 + \sum_{n=0}^{N}\left[G_n|_{\tau_0}\frac{\Delta\tau^n}{n!}\right]\mathbf{v}_0 + \sum_{n=0}^{N}\left[A_n|_{\tau_0}\frac{\Delta\tau^n}{n!}\right]\mathbf{r}_{m_1,0} + \sum_{n=0}^{N}\left[B_n|_{\tau_0}\frac{\Delta\tau^n}{n!}\right]\mathbf{v}_{m_1,0} \\ &\equiv F\mathbf{r}_0 + G\mathbf{v}_0 + A\mathbf{r}_{m_1,0} + B\mathbf{v}_{m_1,0}\end{aligned} \tag{24}$$

The extended Lagrange coefficients form of the solution is:

$$\mathbf{r}(\tau = \tau_0 + \Delta\tau) = f\mathbf{r}_0 + g\mathbf{v}_0 + a\mathbf{r}_{m_1,0} + b\mathbf{v}_{m_1,0} \tag{25}$$

Therefore, taking the decomposition in Eq. (24) to infinity, and comparing it term by term to Eq. (25) yields a relation between the f, g, a, b functions and their associated series:

$$\begin{aligned} f &= \sum_{n=0}^{\infty}\left[F_n|_{\tau_0}\frac{\Delta\tau^n}{n!}\right] \\ g &= \sum_{n=0}^{\infty}\left[G_n|_{\tau_0}\frac{\Delta\tau^n}{n!}\right] \\ a &= \sum_{n=0}^{\infty}\left[A_n|_{\tau_0}\frac{\Delta\tau^n}{n!}\right] \\ b &= \sum_{n=0}^{\infty}\left[B_n|_{\tau_0}\frac{\Delta\tau^n}{n!}\right] \end{aligned} \tag{26}$$

In order to obtain the coefficients of the F and G CRTBP series for any order n, the successive derivatives of $\mathbf{r}$ at τ are decomposed in the basis formed by $\mathbf{r}$, $\mathbf{v}$, $\mathbf{r}_{m_1}$ and $\mathbf{v}_{m_1}$. It is important to note that this decomposition, when evaluated at τ_0, is the one shown in Eq. (23).

$$\frac{d^n \mathbf{r}}{d\tau^n} = F_n\mathbf{r} + G_n\mathbf{v} + A_n\mathbf{r}_{m_1} + B_n\mathbf{v}_{m_1} \tag{27}$$

Equation (27) can be differentiated with respect to τ, using Eq. (15) and Eq. (19):

$$\begin{aligned}\frac{d^{n+1}\mathbf{r}}{d\tau^{n+1}} &= F_n'\mathbf{r} + F_n s\mathbf{v} + G_n'\mathbf{v} + G_n s(p\mathbf{r} + q\mathbf{r}_{m_1}) + A_n'\mathbf{r}_{m_1} + A_n s\mathbf{v}_{m_1} + B_n'\mathbf{v}_{m_1} - B_n s\mathbf{r}_{m_1} \\ &= (F_n' + spG_n)\mathbf{r} + (G_n' + sF_n)\mathbf{v} + (A_n' + sqG_n - sB_n)\mathbf{r}_{m_1} + (B_n' + sA_n)\mathbf{v}_{m_1}\end{aligned} \tag{28}$$

Alternatively, Eq. (27) can be advanced from n to $n+1$:

$$\frac{d^{n+1}\mathbf{r}}{d\tau^{n+1}} = F_{n+1}\mathbf{r} + G_{n+1}\mathbf{v} + A_{n+1}\mathbf{r}_{m_1} + B_{n+1}\mathbf{v}_{m_1} \tag{29}$$

Comparing Eq. (28) and Eq. (29) yields the recursion formulas for F, G, A, and B:

$$\begin{aligned} F_{n+1} &= F'_n + spG_n \\ G_{n+1} &= G'_n + sF_n \\ A_{n+1} &= A'_n + sqG_n - sB_n \\ B_{n+1} &= B'_n + sA_n \end{aligned} \tag{30}$$

As mentioned earlier, a fifth series is necessary in order to integrate the time with respect to τ:

$$\Delta t \simeq \sum_{n=1}^{N} \frac{d^n t}{d\tau^n} \frac{\Delta\tau^n}{n!} = \sum_{n=1}^{N} T_n \frac{\Delta\tau^n}{n!} \tag{31}$$

$$T_{n+1} = T'_n \tag{32}$$

For $\Delta\tau = 0$, $\mathbf{r}(\tau_0) = F_0\mathbf{r}_0 + G_0\mathbf{v}_0 + A_0\mathbf{r}_{m_1,0} + B_0\mathbf{v}_{m_1,0} = \mathbf{r}_0$. The coefficients are therefore initialized using $F_0 = 1$, $G_0 = A_0 = B_0 = 0$. Since $dt/d\tau = s$, $T_0 = 0$, $T_1 = s$.

When using the recursion equations described in Eq. (30) and Eq. (32) at order n, the derivatives of the coefficients of previous orders with respect to τ have to be computed. In order to compute those derivatives in a recursion, a set of new intermediate variables and differentiation rules are necessary. A complete set requires that derivatives of all the variables with respect to τ can be expressed as explicit functions of the variables. The creation of the set is initiated by the differentiation of r_1 and r_2, which appear in p and q, as well as in the Sundman transformation term s.

$$r'_1 = s\frac{\mathbf{r}_1 \cdot \mathbf{v}_1}{r_1} = s\frac{(\mathbf{r} - \mathbf{r}_{m_1}) \cdot (\mathbf{v} - \mathbf{v}_{m_1})}{r_1} = s\frac{\mathbf{r}\cdot\mathbf{v} - \mathbf{r}_{m_1}\cdot\mathbf{v} - \mathbf{r}\cdot\mathbf{v}_{m_1}}{r_1} = s\frac{k_1 - k_2 - k_3}{r_1} \tag{33}$$

$$r'_2 = s\frac{\mathbf{r}_2 \cdot \mathbf{v}_2}{r_2} = s\frac{(\mathbf{r} + c\mathbf{r}_{m_1}) \cdot (\mathbf{v} + c\mathbf{v}_{m_1})}{r_2} = s\frac{\mathbf{r}\cdot\mathbf{v} + c\mathbf{r}_{m_1}\cdot\mathbf{v} + c\mathbf{r}\cdot\mathbf{v}_{m_1}}{r_2} = s\frac{k_1 + c(k_2 + k_3)}{r_2} \tag{34}$$

$$k_1 \equiv \mathbf{r}\cdot\mathbf{v} \qquad k'_1 = s(\mathbf{v}\cdot\mathbf{v} + p\mathbf{r}\cdot\mathbf{r} + q\mathbf{r}\cdot\mathbf{r}_{m_1}) = s(k_4 + pk_5 + qk_6) \tag{35}$$

$$k_2 \equiv \mathbf{r}_{m_1}\cdot\mathbf{v} \qquad k'_2 = s(\mathbf{v}_{m_1}\cdot\mathbf{v} + p\mathbf{r}_{m_1}\cdot\mathbf{r} + q\mathbf{r}_{m_1}\cdot\mathbf{r}_{m_1}) = s\big(k_7 + pk_6 + qr^2_{m_1}\big) \tag{36}$$

$$k_3 \equiv \mathbf{r}\cdot\mathbf{v}_{m_1} \qquad k'_3 = s(\mathbf{v}\cdot\mathbf{v}_{m_1} - \mathbf{r}\cdot\mathbf{r}_{m_1}) = s(k_7 - k_6) \tag{37}$$

$$k_4 \equiv \mathbf{v}\cdot\mathbf{v} \qquad k'_4 = s(2p\mathbf{v}\cdot\mathbf{r} + 2q\mathbf{v}\cdot\mathbf{r}_{m_1}) = 2s(pk_1 + qk_2) \tag{38}$$

$$k_5 \equiv \mathbf{r}\cdot\mathbf{r} \qquad k'_5 = 2s\mathbf{r}\cdot\mathbf{v} = 2sk_1 \tag{39}$$

$$k_6 \equiv \mathbf{r}\cdot\mathbf{r}_{m_1} \qquad k'_6 = s(\mathbf{v}\cdot\mathbf{r}_{m_1} + \mathbf{r}\cdot\mathbf{v}_{m_1}) = s(k_2 + k_3) \tag{40}$$

$$k_7 \equiv \mathbf{v}\cdot\mathbf{v}_{m_1} \qquad k'_7 = s(p\mathbf{r}\cdot\mathbf{v}_{m_1} - \mathbf{v}\cdot\mathbf{r}_{m_1}) = s(pk_3 - k_2) \tag{41}$$

Using the recursive Equations (30) and (32) with the intermediate results from Eq. (33) to (41), the coefficients of the five F and G CRTBP series can be computed up to arbitrary order N and are evaluated at $\tau = \tau_0$. Then, Eq. (24) is used to obtain the position vector $\mathbf{r}$. In order to compute the velocity vector $\mathbf{v}$, Eq. (24) is differentiated with respect to time:

$$\begin{aligned} \mathbf{v} &= \frac{d\mathbf{r}}{dt} = \frac{d\mathbf{r}}{d\tau}\frac{d\tau}{dt} = \frac{1}{s}\mathbf{r}' \\ &= \frac{1}{s}\left(\sum_{n=1}^{N}\left[F_n|_{\tau_0}\frac{\Delta\tau^{n-1}}{(n-1)!}\right]\mathbf{r}_0 + \sum_{n=1}^{N}\left[G_n|_{\tau_0}\frac{\Delta\tau^{n-1}}{(n-1)!}\right]\mathbf{v}_0\right. \\ &\qquad \left. + \sum_{n=1}^{N}\left[A_n|_{\tau_0}\frac{\Delta\tau^{n-1}}{(n-1)!}\right]\mathbf{r}_{m_1,0} \sum_{n=1}^{N}\left[B_n|_{\tau_0}\frac{\Delta\tau^{n-1}}{(n-1)!}\right]\mathbf{v}_{m_1,0}\right) \end{aligned} \tag{42}$$

The relations presented in this section are implemented via the symbolic manipulation software Maple 17. The code generation capability of Maple is used to generate optimized Fortran code. More information on

the implementation can be found in Ref. 19. As for the solution to the Stark problem,[19] the main drawback of this technique is the increasing complexity of the terms of high order. The chain rules involved in the successive differentiations lead to large coefficient files, as the symbolic manipulator and compiler become overwhelmed for high orders. This practical limitation on the order N explains the maximum orders (12 - 15 depending on the independent variable definition) chosen in Section 3.

3 NUMERICAL RESULTS

This section presents the results of the Taylor series integration for different scenarios. The method is validated, and its performance is compared to that of a conventional eighth order Runge-Kutta-Fehlberg integrator. Both variable-step and fixed-step integrations are considered and compared. The Sundman type transformations are used for the fixed-step integration, and the behavior of the associated solutions is studied. In all plots, the F and G solutions are not all computed up to the same order, due to the varying complexity induced by the different Sundman transformations. The maximum orders are: 15 with no Sundman transformation, 13 in the $s = r_1$ and $s = r_2$ cases, and 12 in the $s = r_1 r_2$ case. All timing results are sensitive to implementation choices and compilation settings; however, a good-faith effort was made by the authors to ensure fair comparisons of the integration methods. The timings are obtained using the intrinsic Fortran routine `cpu_time`, and averaging over $10,000$ simulations. Four different scenarios have been considered in this study, in order to qualitatively capture the different types of motion in the CRTBP. The scenarios are four periodic orbits presented in Subsection 3.1. In each case, the periodic orbit is propagated for one period.

The results presented in this section are obtained using the GNU Fortran compiler (gfortran) v4.7.0 on a Windows 7 workstation with a quad-core Intel Xeon W3550 CPU with 3.07GHz clock speed, and 6GB of RAM. The `-O3` optimization flag was used during compilation. The coefficient files are generated using Maple 17.

3.1 Framework: considered system and scenarios

The CRTBP studied in the present paper is a representation of the Earth-Moon system, with the mass ratio $\mu = 1/82.27 = 0.012155099064057$ given by Broucke in Ref. 30. The distance between the two masses is the Earth-Moon distance (384400 km $= 1$ LU). The initial conditions for the primary are:

$$\left[x_0 \; y_0 \; z_0 \; \dot{x}_0 \; \dot{y}_0 \; \dot{z}_0\right]_{m_1}^T = \left[-\mu \,\text{LU},\; 0\,\text{LU},\; 0\,\text{LU},\; 0\,\text{LU/TU},\; -\mu\,\text{LU/TU},\; 0\,\text{LU/TU}\right]^T \tag{43}$$

This section presents the four different scenarios studied in this paper. The first three scenarios are planar periodic orbits, with initial conditions found in Ref. 30, and the fourth one is a 3D Halo orbit found using differential correction. In Scenario 1, the particle orbits the primary m_1. In Scenario 2, the particle stays close to m_2. In Scenario 3, the particle goes back and forth between m_2 and m_1. Table 1 contains the initial conditions for each orbit, as well as their period, and the distance of their closest approach to each mass. Figures 2 to 5, in addition to presenting the studied trajectories, show the influence of the Sundman transformations in each case. Time is effectively "slowed down" when the particle approaches one of the masses, allowing for a more robust integration, in particular for a fixed-step integrator. Subsection 3.3 confirms the utility of the Sundman type transformations. Figures 2 to 5 are obtained using the fixed-step twelfth order F and G solution, with the minimum number of steps required so that $\epsilon_f \leq 10^{-6}$ (see Subsection 3.2 and Subsection 3.3). Not all integration steps are shown, and the spacing between shown integration steps is displayed on the plot. Figure 5 is a plot of the 3D Halo trajectory, and of the projections of this 3D trajectory on the (x, y), (y, z), and (x, z) planes.

Table 1: Initial conditions for the four test scenarios

	Scenario 1	Scenario 2	Scenario 3	Scenario 4
x_0 (LU)	-1.972795736	1.044045197	0.960920244	0.974785880885315
y_0 (LU)	0.0	0.0	0.0	0.0
z_0 (LU)	0.0	0.0	0.0	0.071295151958740
$\dot{x}_0$ (LU/TU)	0.0	0.0	0.0	0.0
$\dot{y}_0$ (LU/TU)	1.864677641	-0.633046910	-0.958491618	-0.526306975588415
$\dot{z}_0$ (LU/TU)	0.0	0.0	0.0	0.0
T_P (TU)	6.283185420	6.283159790	18.489999998	2.517727406553485
Min. dist. to m_1 (LU)	0.02236542879	0.83006201718	0.36743999383	0.88258730021
Min. dist. to m_2 (LU)	0.59037482616	0.03951491160	0.02690767703	0.07248128515

Scenario 1 is Orbit 33 on Table 3 of Ref. 30
Scenario 2 is Orbit 65 on Table 9 of Ref. 30
Scenario 3 is Orbit 263 on Table 5 of Ref. 30
Scenario 4 is obtained using a differential corrector and well known techniques for finding Halo orbits
Earth radius $R_E = 0.01659$ LU ; Moon radius $R_M = 0.004519$ LU

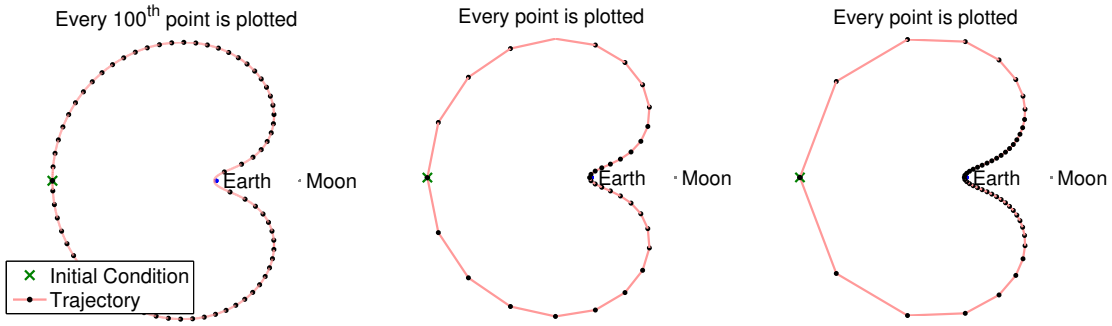

(a) Scenario 1, $s = 1$ (b) Scenario 1, $s = r_1$ (c) Scenario 1, $s = r_1 r_2$

Figure 2: Scenario 1, with different Sundman transformations $\epsilon_f \leq 10^{-6}$

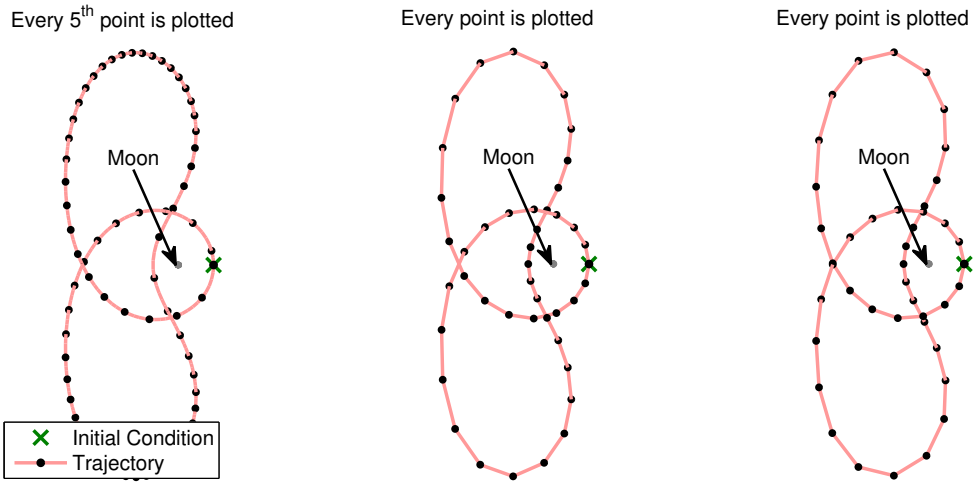

(a) Scenario 2, $s = 1$ (b) Scenario 2, $s = r_2$ (c) Scenario 2, $s = r_1 r_2$

Figure 3: Scenario 2, with different Sundman transformations $\epsilon_f \leq 10^{-6}$

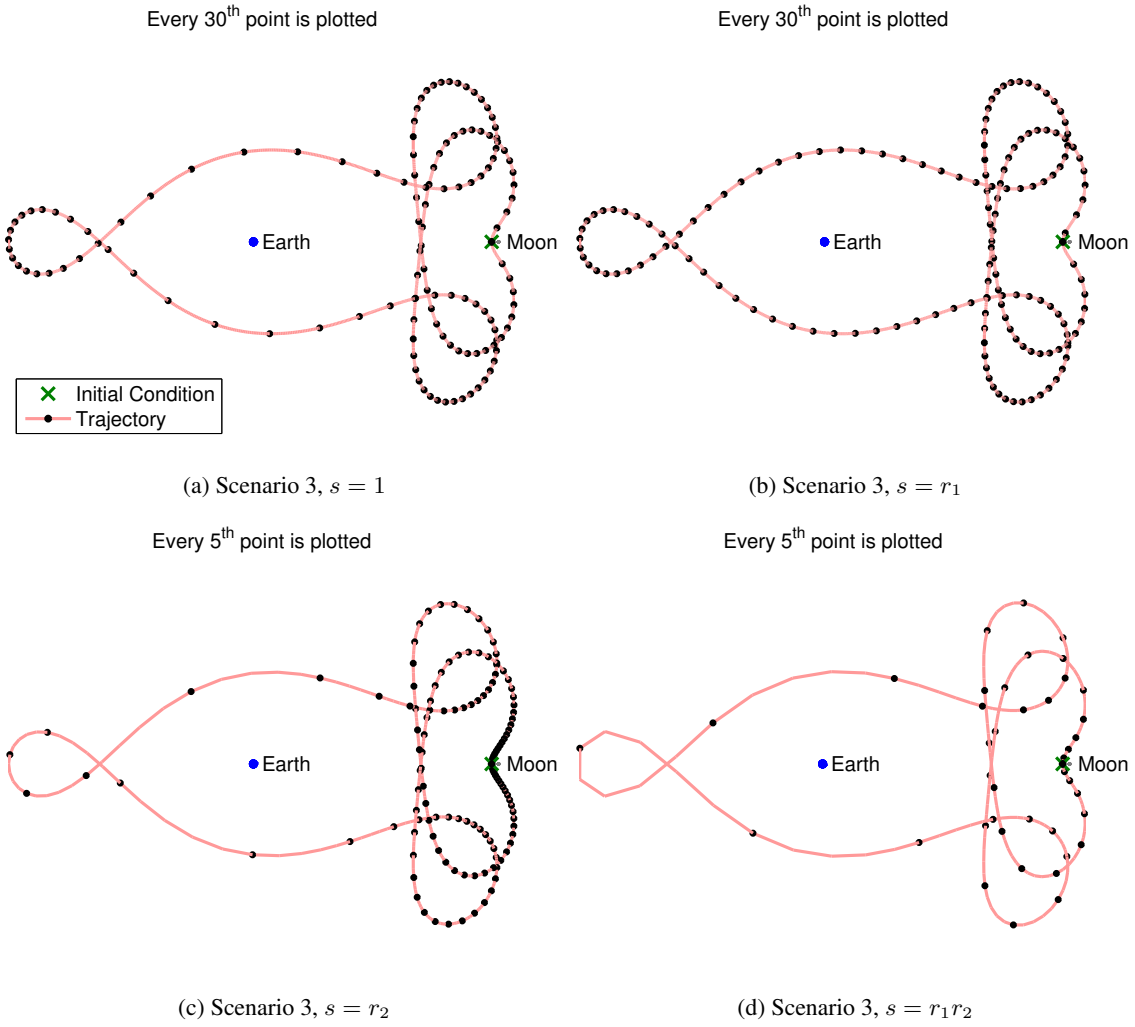

(a) Scenario 3, $s = 1$

(b) Scenario 3, $s = r_1$

(c) Scenario 3, $s = r_2$

(d) Scenario 3, $s = r_1 r_2$

Figure 4: Scenario 3, with different Sundman transformations $\epsilon_f \leq 10^{-6}$

3.2 Variable-step integration

The four scenarios are integrated using variable-step integration methods. The F and G CRTBP series solution is compared to a conventional RKF(7)8. In the case of the series solution, the error estimate, necessary to adjust the step-size, is given by the infinity norm of the last vector added to the series. For order N, the estimate of the error is:

$$\epsilon = \| \begin{bmatrix} \boldsymbol{\epsilon}_r^T & \boldsymbol{\epsilon}_v^T & \boldsymbol{\epsilon}_T^T \end{bmatrix}^T \|_\infty \tag{44}$$

$$\boldsymbol{\epsilon}_r = \left(F_N|_{\tau_0} \mathbf{r}_0 + G_N|_{\tau_0} \mathbf{v}_0 + A_N|_{\tau_0} \mathbf{r}_{m_1,0} + B_N|_{\tau_0} \mathbf{v}_{m_1,0} \right) \frac{\Delta\tau^N}{N!} \tag{45}$$

$$\boldsymbol{\epsilon}_v = \frac{1}{s} \left(F_N|_{\tau_0} \mathbf{r}_0 + G_N|_{\tau_0} \mathbf{v}_0 + A_N|_{\tau_0} \mathbf{r}_{m_1,0} + B_N|_{\tau_0} \mathbf{v}_{m_1,0} \right) \frac{\Delta\tau^{N-1}}{(N-1)!} \tag{46}$$

$$\boldsymbol{\epsilon}_t = T_N|_{\tau_0} \frac{\Delta\tau^N}{N!} \tag{47}$$

This error estimate is used in the variable-step integrator in a manner similar to the Runge-Kutta variable-step integrators.[31] The user inputs an absolute (ϵ_a) and a relative (ϵ_{rel}) tolerance, and at each step the algorithm

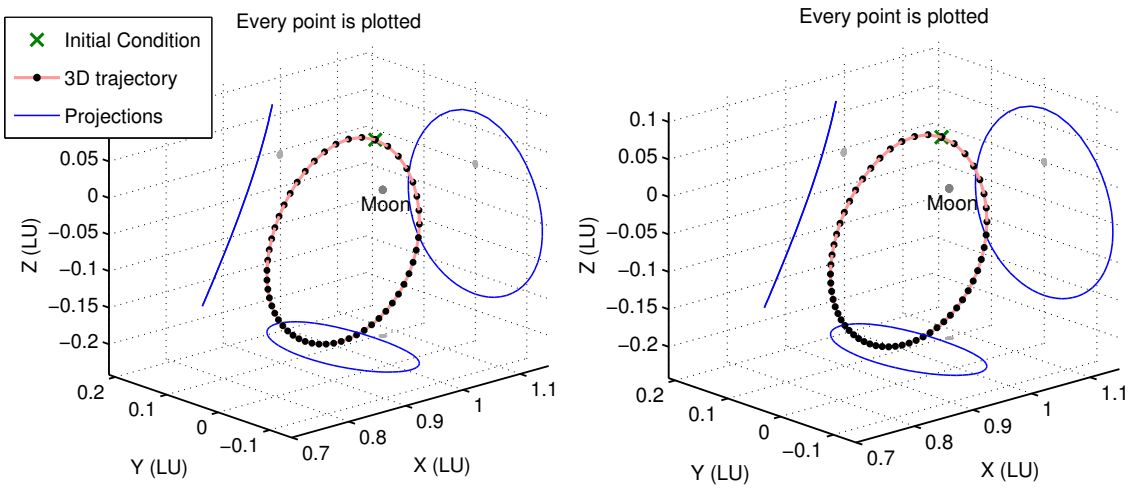

(a) Scenario 4, $s = 1$

(b) Scenario 4, $s = r_1$

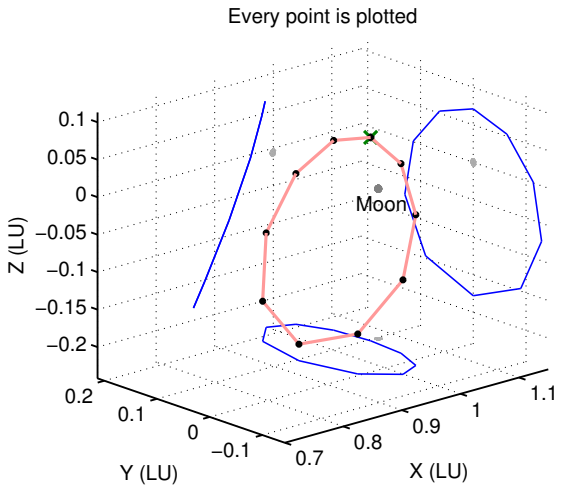

(c) Scenario 4, $s = r_2$

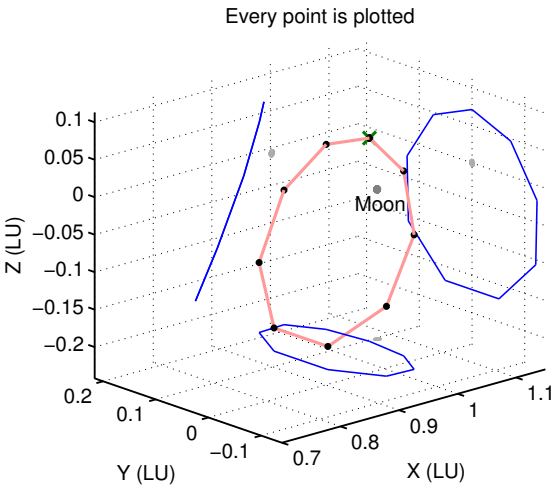

(d) Scenario 4, $s = r_1 r_2$

Figure 5: Scenario 4, with different Sundman transformations $\epsilon_f \leq 10^{-6}$

ensures that:

$$\epsilon \leq \max(\epsilon_a, \epsilon_{\text{rel}} \|\mathbf{X}\|_\infty) \tag{48}$$

In the following, the tolerances are set such that $\epsilon_a = \epsilon_{\text{rel}}$, and only ϵ_a is mentioned.

In order to compare the time required by different integration routines, it is important to ensure that similar accuracies are obtained in each case. In the current paper, the accuracy ϵ_f is defined as the norm of the difference between the truth and the state vector at the final time of integration, as shown in Eq. (49). The truth is computed using a variable-step RKF(7)8 in quad precision, with tolerance $\epsilon_a = 10^{-22}$.

$$\epsilon_f = \|\mathbf{X}(\tau_f)_{\text{TRUTH}} - \mathbf{X}(\tau_f)\| \tag{49}$$

To ensure a fair comparison of methods, the prescribed error tolerance ϵ_a for each integrator is successively reduced, until the accuracy ϵ_f described in Eq. (49) steps below a prescribed error threshold (ϵ_{thresh}). This comparison scheme not only controls the local error (an inherent feature of the variable-step algorithms), it

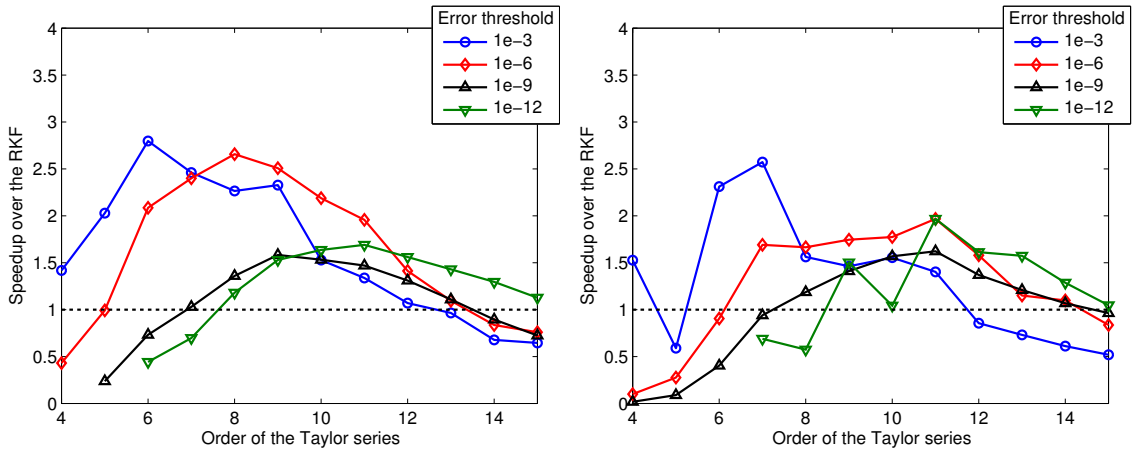

(a) Speedups for Scenario 1

(b) Speedups for Scenario 2

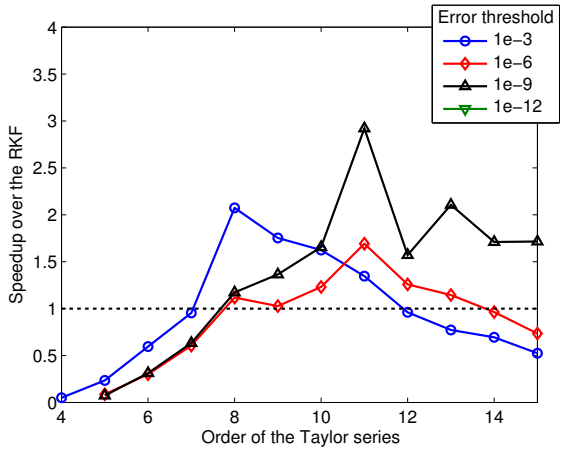

(c) Speedups for Scenario 3. For $\epsilon_{thresh} = 10^{-12}$, neither the F and G series nor the RKF converged

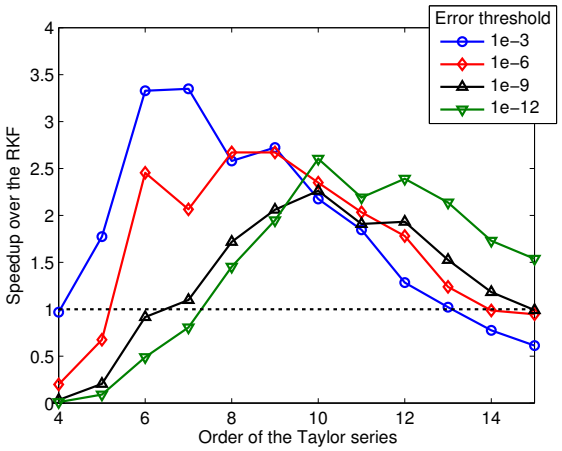

(d) Speedups for Scenario 4

Figure 6: Speedups of the variable-step F and G CRTBP propagator compared to the RKF(7)8. No Sundman transformation is used ($s = 1$)

also ensures that the final accuracies are comparable. Moreover, slowly reducing ϵ_a ensures that ϵ_{thresh} is reached while minimizing the computational efforts necessary to achieve it.

Figure 6 presents the speedups obtained when comparing the variable-step F and G CRTBP solution to the variable-step RKF(7)8 for each scenario. No time transformation is used for the variable-step propagation ($s = 1$). The results are given for different error thresholds (ϵ_{thresh}). Missing data points correspond to cases where the lower-order F and G series did not converge even for the lowest possible value of ϵ_a ($\epsilon_a = 10^{-16}$).

The behavior of the variable-step F and G integration presented in Fig. 6 is similar for all four scenarios. The F and G Taylor series solution is up to $3.3\times$ faster than the RKF(7)8. Moreover, for low-fidelity propagations ($\epsilon_{thresh} = 10^{-3}$), the F and G series are between two and three times faster than the RKF(7)8 for all test cases, when selecting an appropriate order. This speedup makes the F and G series an attractive integrator for preliminary trajectory design using the CRTBP. The results of Fig. 6 are consistent with previously published comparisons between power series solutions of the CRTBP and Runge-Kutta integration: Jorba and Zou[14] demonstrate that their power series solution to the CRTBP performs up to three times faster than a Runge-Kutta integration. For every propagation, an optimal order can be observed. In general, as

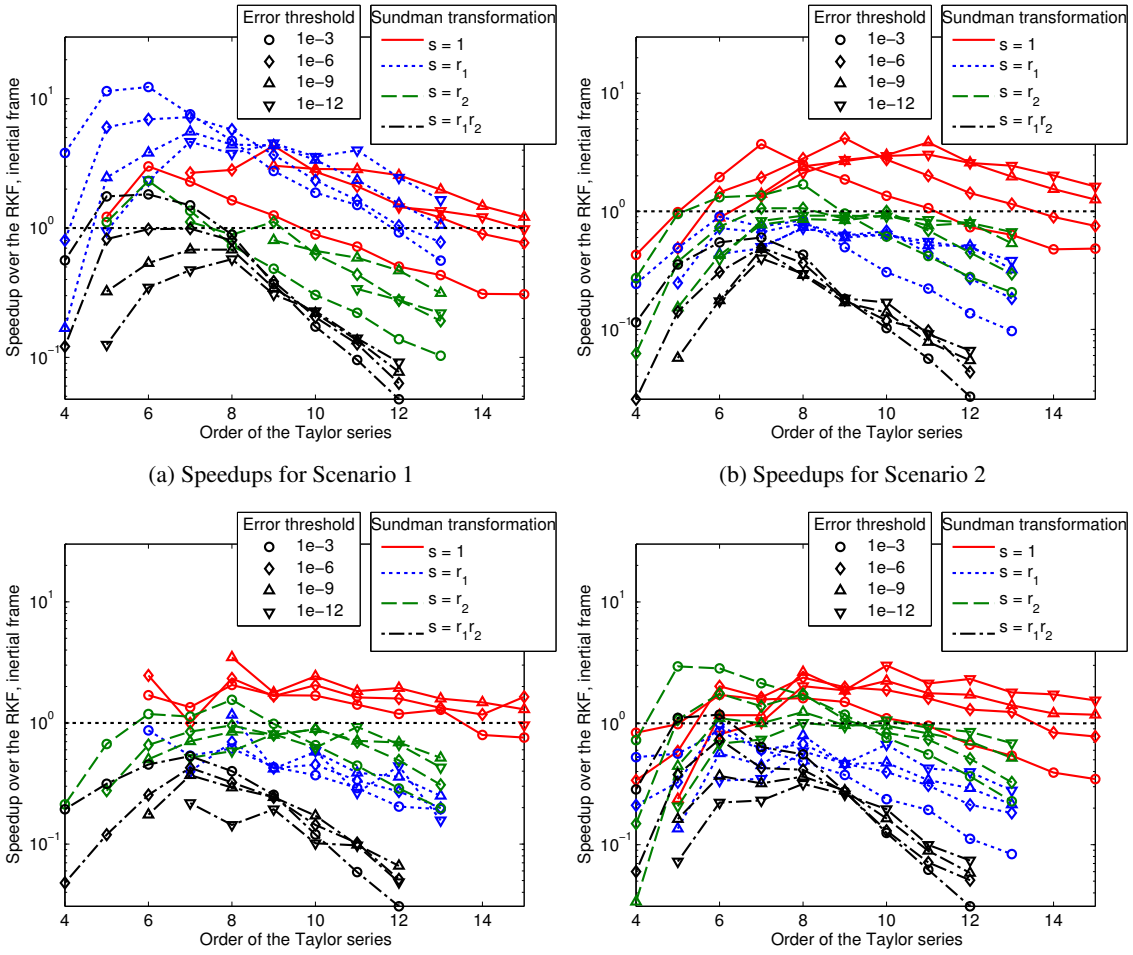

(a) Speedups for Scenario 1

(b) Speedups for Scenario 2

(c) Speedups for Scenario 3

(d) Speedups for Scenario 4

Figure 7: Speedups of the fixed-step F and G CRTBP propagator compared to the RKF8

the prescribed error threshold is lowered, the optimal order increases, corresponding to an increased need of precision.

3.3 Fixed-step integration

Comparisons of the fixed-step integrators are performed under conditions similar to the variable-step comparisons. The accuracy is the one described in Eq. (49), and the comparison scheme also relies on bringing this accuracy below a prescribed error threshold ϵ_{thresh}. However, in order to reach ϵ_{thresh}, the number of steps taken by the algorithm is slowly increased, instead of lowering the tolerance ϵ_a. This similarly ensures that ϵ_{thresh} is reached while minimizing the computational efforts.

Figure 7 presents the speedups obtained when comparing the fixed-step F and G CRTBP solution to the fixed-step RKF8. The results are given for different ϵ_{thresh} and for the different Sundman transformations presented in Subsection 2.2. Figure 8 shows the number of steps necessary to achieve the prescribed error threshold $\epsilon_{\text{thresh}} = 10^{-6}$ for each method, and for the different Sundman transformations. Two different orders of the F and G solutions are presented.

Figure 7 exhibits a behavior of the fixed-step F and G integration similar to that of the variable-step integration. The Taylor series solution presents a different optimal order for each error threshold, increasing

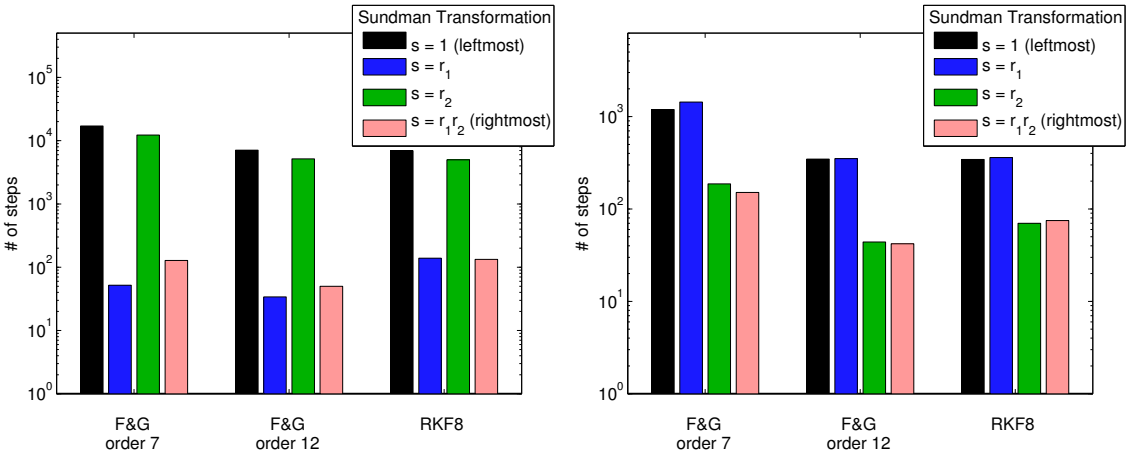

(a) Scenario 1

(b) Scenario 2

(c) Scenario 3

(d) Scenario 4

Figure 8: Number of steps necessary to achieve the prescribed tolerance $\epsilon_{\text{thresh}} = 10^{-6}$ using fixed-step integration

as the threshold is lowered. The speedups over the RKF8 go as high as $13\times$. The Sundman transformation usually lowers the speedups, indicating that the RKF8 benefits most from the regularization. This change in relative performance when using a Sundman transformation has two sources: 1) the Sundman tranformations result in an increase in the complexity of the equations of motion, and associated recursion expressions. 2) the Sundman transformation reduces the number of steps necessary for convergence and accelerates the RKF8 integration.

Figure 8 confirms these tendencies: the number of necessary integration steps is greatly reduced when using an adapted Sundman transformation, for every integration method. As expected based on the proximity of the trajectories to each primary, the best transformations are $s = r_1$ for Scenario 1, $s = r_2$ for Scenarios 2 and 4, and $s = r_1 r_2$ for Scenario 3. However, in all cases the difference between the ideal transformation and the $s = r_1 r_2$ is relatively small, making the $s = r_1 r_2$ transformation the most useful across all cases. Up to two orders of magnitude fewer steps are necessary to converge when using the $s = r_1 r_2$ transformation, compared to the time propagation. As noted, the effect of the regularization on the minimum number of steps are comparable for each method; the resulting speedups are explained by the much increased complexity of the coefficient files of the Taylor series.

4 CONCLUSION

In this paper, a new integration method for the CRTBP, based on the Lagrange coefficients and their associated Taylor series, is developed. The CRTBP equations of motion are extended to include a Sundman type transformation for efficient discretization. Exact recursion formulas for the obtention of the coefficients of the Taylor series are presented. The resulting coefficient files are generated using a symbolic manipulator and can be downloaded in the form of Fortran subroutines from `http://russell.ae.utexas.edu/index_files/fgcrtbp.htm`.

The method is validated on four different test cases designed to represent different orbit classes of the CRTBP, in both 2D and 3D. The computational performance of the F and G solution is compared to that of an eighth order RKF integrator and both variable-step and fixed-step integrations are studied. The overall performance of the F and G Taylor series solutions is comparable to that of the conventional numerical integrator, when considering all the parameters above. The results are consistent with a previous study comparing a Modern Taylor Series (Taylor series with Automatic Differentiation) integration method to an RKF8, implying that the F and G method is qualitatively similar in performance to power series methods. In addition, the variable-step F and G series with no time transformation are demonstrated to perform between two and three times faster than the conventional RKF(7)8 for low-fidelity propagations, making them particularly useful for preliminary design of three-body trajectories.

The Sundman transformations are demonstrated to improve the discretization of the orbit and lower the number of steps necessary for convergence of the algorithms. The "hybrid" Sundman transformation, regularizing the equations of motion at both primaries, is shown to have the most satisfactory results across all test cases. It allows a reduction of the number of necessary integration steps over the time propagation, for all test cases, and for all methods. However, the regularizations increase the complexity of the equations of motion, and therefore of the Taylor series computation, slowing down the F and G method. On the other hand, the RKF performs particularly well under the transformations, suggesting the utility of fixed-step RKF integrators using Sundman transformed CRTBP equations of motion. Such an implementation is not common in practice, but the analysis in this study gives evidence of its benefit.

5 ACKNOWLEDGMENT

This work was supported in part by a NASA Research Announcement/Research Opportunities in Space and Earth Sciences award (No. NNX13AH04G). The authors thank John Dankanich for his interest and support.

REFERENCES

[1] G. Gomez, W. S. Koon, M. W. LO, J. E. Marsden, J. Masdemont, and S. D. Ross, "Invariant Manifolds, the Spatial Three-Body Problem and Space Mission Design," *Advances in Astronautical Sciences*, Vol. 109, 2001, pp. 3–22.

[2] R. L. Anderson and M. W. Lo, "Flyby Design using Heteroclinic and Homoclinic Connections of Unstable Resonant Orbits," *AAS/AIAA Spaceflight Mechanics Meeting*, 2011.

[3] G. Lantoine and R. P. Russell, "Near Ballistic Halo-to-Halo Tranfers between Planetary Moons," *The Journal of the Astronautical Sciences*, Vol. 58, No. 3, 2011, pp. 335–363. doi:10.1007/BF03321174.

[4] V. G. Szebehely, *Theory of Orbits, The Circular Restricted Three-Body Problem*. New York, NY: Academic Press, 1967.

[5] K. Fox, "Numerical Integration of the Equations of Motion of Celestial Mechanics," *Celestial Mechanics*, Vol. 33, No. 2, 1984, pp. 127–142. doi:10.1007/BF01234151.

[6] O. Montenbruck, "Numerical Integration Methods for Orbital Motion," *Celestial Mechanics and Dynamical Astronomy*, Vol. 53, 1992, pp. 59 – 69. doi:10.1007/BF00049361.

[7] O. Montenbruck, "Numerical Integration of Orbital Motion using Taylor Series," *AAS/AIAA Spaceflight Mechanics Conference*, Colorado Springs, CO, AAS, 1992.

[8] E. Fehlberg, "Numerical Integration of Differential Equations by Power Series Expansion," tech. rep., NASA TN D-2356, 1964.

[9] J. F. Steffensen, "On the Restricted Problem of Three Bodies," *Kongelige Danske Videnskabernes Selskab Mat.-Fys. Medd.*, Vol. 30, No. 18, 1956.

[10] E. Rabe, "Determination and Survey of Periodic Trojan Orbits in the Restricted Problem of Three Bodies," *The Astronomical Journal*, Vol. 66, No. 9, 1961, pp. 500 – 513. doi:10.1086/108451.

[11] A. Deprit and J. F. Price, "The Computation of Characteristic Exponents in the Planar Restricted Problem of Three Bodies," *The Astronomical Journal*, Vol. 70, No. 10, 1965. doi:10.1086/109823.

[12] R. Broucke, "Stability of periodic orbits in the elliptic, restricted three-body problem.," *AIAA Journal*, Vol. 7, June 1969, pp. 1003–1009. doi:10.2514/3.5267.

[13] A. Deprit and R. V. M. Zahar, "Numerical Integration of an Orbit and Its Concomitant Variations by Recurrent Power Series," *Zeitschrift für angewandte Mathematik und Physik ZAMP*, Vol. 17, No. 3, 1966, pp. 425–430. doi:10.1007/BF01594535.

[14] A. Jorba and M. Zou, "A Software Package for the Numerical Integration of ODEs by Means of High-Order Taylor Methods," *Experimental Mathematics*, Vol. 14, No. 1, 2005, pp. 99–117. doi:10.1080/10586458.2005.10128904.

[15] R. R. Bate, D. D. Mueller, and J. E. White, *Fundamentals of Astrodynamics*. New-York, NY: Dover Publications, 1971.

[16] P. Sconzo, A. LeSchack, and R. Tobey, "Symbolic Computation of f and g Series by Computer," *The Astronomical Journal*, Vol. 70, No. 4, 1965, pp. 269 – 270. doi:10.1086/109718.

[17] V. R. Bond, "A Recursive Formulation for Computing the Coefficients of the Time-Dependent f and g Series Solutions to the Two-Body Problem," *The Astronomical Journal*, Vol. 71, No. 1, 1966, pp. 7–8. doi:10.1086/109845.

[18] D. N. Papadakos, "Generalized F and G Series and Convergence of the Power Series Solution to the N-Body Problem," *Celestial Mechanics*, Vol. 30, No. 1, 1983, pp. 275–282. doi:10.1007/BF01232193.

[19] E. Pellegrini, R. P. Russell, and V. Vittaldev, "F and G Taylor Series Solutions to the Stark and Kepler Problems with Sundman Transformations," *Celestial Mechanics and Dynamical Astronomy*, *to appear*. doi:10.1007/s10569-014-9538-7.

[20] K. F. Sundman, "Mémoire sur le problème des trois corps," *Acta Mathematica*, Vol. 36, Dec. 1912, pp. 105–179. doi:10.1007/BF02422379.

[21] G. D. Birkhoff, "The Restricted Problem of Three Bodies," *Rend. Circ. Mat. Palermo*, Vol. 39, No. 1, 1915.

[22] G. Lemaitre, "Regularization of the Three Body Problem," *Vistas in Astronomy*, Vol. 1, 1955, p. 207. doi:10.1016/0083-6656(55)90028-3.

[23] T. N. Thiele, "Recherche numerique concernant des solutions periodiques d'un cas special du probleme des trois corps," *Astron. Nachr.*, Vol. 138, No. 1, 1896.

[24] C. Burrau, "Uber einige in Aussicht genommene Berechnung, betreffend einen Spezialfall des Dreikorperproblems," *Vierteljahrsschrift Astron. Ges.*, Vol. 41, 1906.

[25] G. J. Whiffen, "Mystic: Implementation of the Static Dynamic Optimal Control Algorithm for High-Fidelity, Low-Thrust Trajectory Design," *AIAA/AAS Astrodynamics Specialists Conference*, 2006. doi:10.2514/6.2006-6741.

[26] V. G. Szebehely and F. Peters, "Complete Solution of a General Problem of Three Bodies," *The Astronomical Journal*, Vol. 72, No. 7, 1967, pp. 876 – 883. doi:10.1086/110355.

[27] M. M. Berry and L. M. Healy, "The generalized Sundman transformation for propagation of high-eccentricity elliptical orbits," *Advances in the Astronautical Sciences*, Vol. 112, Jan. 2002, pp. 127–146.

[28] C. H. Yam, D. Izzo, and F. Biscani, "Towards a High Fidelity Direct Transcription Method for Optimisation of Low-Thrust Trajectories," *4th International Conference on Astrodynamics Tools and Techniques*, 2010, pp. 1–7.

[29] T. Levi-Civita, "Sur la Regularisation du Probleme des Trois Corps," *Acta Mathematica*, Vol. 42, 1920, pp. 99–144. doi:10.1007/BF02404404.

[30] R. Broucke, "Periodic Orbits in the Restricted Three-Body Problem with Earth-Moon Masses," tech. rep., Jet Propulsion Laboratory, Pasadena, California, 1968.

[31] W. H. Press, S. A. Teukolsky, W. T. Vetterling, and B. P. Flannery, *Numerical Recipes in Fortran 77: the Art of Scientific Computing*. Cambridge University Press, 1992.